Analytical Biochemistry 418 (2011) 247–252

Contents lists available at SciVerse ScienceDirect

Analytical Biochemistry

journal homepage: www.elsevier.com/locate/yabio

Sensitive fluorogenic substrate for alkaline phosphatase

Michael N. Levine [a], Ronald T. Raines [a,b,*]

[a] Department of Biochemistry, University of Wisconsin–Madison, Madison, WI 53706, USA
[b] Department of Chemistry, University of Wisconsin–Madison, Madison, WI 53706, USA

ARTICLE INFO

Article history:
Received 21 May 2011
Received in revised form 10 July 2011
Accepted 18 July 2011
Available online 24 July 2011

Keywords:
Alkaline phosphatase
ELISA
Latent fluorophore
Rhodamine
Trimethyl lock

ABSTRACT

Alkaline phosphatase serves both as a model enzyme for studies on the mechanism and kinetics of phosphomonoesterases and as a reporter in enzyme-linked immunosorbent assays (ELISAs) and other biochemical methods. The tight binding of the enzyme to its inorganic phosphate product leads to strong inhibition of catalysis and confounds measurements of alkaline phosphatase activity. We have developed an alkaline phosphatase substrate in which the fluorescence of rhodamine is triggered on P–O bond cleavage in a process mediated by a "trimethyl lock." Although this substrate requires a nonenzymatic second step to manifest fluorescence, we demonstrated that the enzymatic first step limits the rate of fluorogenesis. The substrate enables the catalytic activity of alkaline phosphatase to be measured with high sensitivity and accuracy. Its attributes are ideal for enzymatic assays of alkaline phosphatase for both basic research and biotechnological applications.

Alkaline phosphatase (EC 3.1.3.1) is a prototypical phosphomonoesterase [1–3] that is used often in enzyme-linked immunosorbent assays (ELISAs)[1] and other biochemical methods [4]. Despite its frequent study and widespread use, determining rate constants for catalysis by alkaline phosphatase is difficult. This difficulty arises largely from the high affinity of alkaline phosphatase for its product, inorganic phosphate. For example, the well-known enzyme from *Escherichia coli* is inhibited with $K_i \approx 1$ μM [5]. In typical spectrophotometric assays for alkaline phosphatase, the concentration of inorganic phosphate saturates the enzyme before a measurable signal is observable, thereby limiting accuracy. Fluorometric assays using aryl phosphates can overcome this limitation. Still, known fluorogenic substrates, such as fluorescein diphosphate [6], are hampered by chemical instability, two-hit kinetics, and pH-dependent fluorescence [7].

Rhodamine 110 is a xanthene dye first synthesized by Maurice Ceresole more than a century ago [8]. Its fluorescence is bright and pH-insensitive, and its emission and excitation wavelengths are ideal for biological assays [9]. To adapt rhodamine 110 as a reporter of enzymatic catalysis, we have employed the "trimethyl lock" as a trigger that couples fluorescence generation to a designated chemical reaction [10–13]. The trimethyl lock is an *o*-hydroxydihydrocinnamic acid derivative in which steric interactions among three methyl groups lead to rapid lactonization to a dihydrocoumarin ring (**3**, Scheme 1) with concomitant release of an alcohol or amine [14–16]. The scission of a labile bond to the phenolic oxygen enables the manifestation of fluorescence [10–13]. Here we describe how the trimethyl lock can enable the fluorescence of rhodamine 110 to report on P–O bond cleavage catalyzed by alkaline phosphatase.

Materials and methods

Materials

Dichloromethane was drawn from a J.T. Baker CYCLE-TAINER solvent delivery system. All other reagents were obtained from Aldrich Chemical (Milwaukee, WI, USA) or Fisher Scientific (Hanover Park, IL, USA) and were used without further purification.

Thin-layer chromatography was performed by using aluminum-backed plates, coated with silica gel containing F_{254} phosphor, and was visualized by ultraviolet illumination or developed with ceric ammonium molybdate stain. Flash chromatography was performed on open columns with Silica Gel 60 (230–400 mesh).

Nuclear magnetic resonance (NMR) spectra were obtained with a Bruker DMX-400 Avance spectrometer at the National Magnetic Resonance Facility at Madison (NMRFAM). Mass spectrometry was performed using a Micromass LCT (electrospray ionization, ESI) mass spectrometer at the Mass Spectrometry Center in the Department of Chemistry University at the University of Wisconsin–Madison.

* Corresponding author at: Department of Biochemistry, University of Wisconsin–Madison, Madison, WI 53706, USA. Fax: +1 608 890 2583.
E-mail address: rtraines@wisc.edu (R.T. Raines).

[1] *Abbreviations used:* ELISA, enzyme-linked immunosorbent assay; NMR, nuclear magnetic resonance; ESI, electrospray ionization; TLC, thin-layer chromatography; DMSO, dimethyl sulfoxide.

0003-2697/$ - see front matter © 2011 Elsevier Inc. All rights reserved.
doi:10.1016/j.ab.2011.07.021

*Synthesis of substrate **1***

3-[2′-(Dibenzylphophono)oxy-4′,6′-dimethylphenyl]-3,3-dimethylpropionic acid [16] (**5** in Scheme 2, 326 mg, 0.676 mmol) was dissolved in anhydrous CH_2Cl_2 (2.0 ml) in a flame-dried, 25-ml round-bottom flask. 1-Chloro-*N*,*N*,2-trimethylpropenylamine (98 μl, 0.75 mmol) in CH_2Cl_2 (0.4 ml) was added quickly, and the reaction mixture was stirred under Ar(g) for 3 h. The reaction progress was followed by thin-layer chromatography (TLC, 50% [v/v] EtOAc in hexanes) after quenching a small aliquot with MeOH to generate the methyl ester. Rhodamine **4** [11] (150 mg, 0.34 mmol) and anhydrous pyridine (109 μl, 1.35 mmol) were dissolved in CH_2Cl_2 (2.0 ml), and the resulting solution was added to the reaction mixture, which was then stirred overnight. The reaction mixture was partitioned between CH_2Cl_2 and water. The organic layer was washed with 50 ml of 1 N HCl, water, 5% (w/v) sodium bicarbonate, water, and brine. The organic phase was dried over Na_2SO_4(s) and filtered, and the solvent was removed under reduced pressure. The residue was purified by silica gel chromatography (7:2:1 EtOAc/CH_2 Cl_2/hexanes), followed by a second column (7:2:1 EtOAc/CH_2Cl_2/toluene) to give phosphotriester **6** as a white solid (161 mg; 52%). ^{1}H NMR (400 MHz, $CDCl_3$) δ: 8.86 (s, 1H), 7.98 (d, J = 7.3 Hz, 1H), 7.63 (ddd, J = 8.3, 7.1, 1.0 Hz, 1H), 7.58 (ddd, J = 8.3, 7.5, 1.1 Hz, 1H), 7.50 (d, J = 1.8 Hz, 1H), 7.40 (d, J = 2.2 Hz, 1H), 7.37–7.34 (m, 10H), 7.09 (d, J = 7.6 Hz, 1H), 6.94 (dd, J = 8.7, 1.8 Hz, 1H), 6.90 (s, 1H), 6.84 (dd, J = 8.8, 1.8 Hz, 1H), 6.67 (s, 1H), 6.64 (d, J = 8.6 Hz, 1H), 6.63 (s, 1H), 6.55 (d, J = 8.7 Hz, 1H), 5.21–5.09 (m, 4H), 3.73 (t, J = 4.7 Hz, 4H), 3.49 (t, J = 4.6 Hz, 4H), 2.72 (d, J = 13.0 Hz, 1H), 2.65 (d, J = 12.9 Hz, 1H), 2.43 (s, 3H), 2.09 (s, 3H), 1.68 (s, 3H), 1.66 ppm (s, 3H). ^{13}C NMR (400 MHz, $CDCl_3$) δ: 170.7, 169.9, 154.7, 153.4, 152.0, 151.7, 150.2, 141.2, 140.9, 139.6, 137.0, 135.1, 135.0, 132.5, 132.2, 129.8, 129.1, 128.9, 128.8, 128.5, 128.4, 128.3, 128.1, 126.6, 125.0, 124.2, 119.5, 115.6, 115.4, 113.4, 113.2, 107.6, 107.4, 83.3, 70.6, 66.6, 50.1, 44.4, 41.0, 32.4, 25.8, 20.4 ppm. ^{31}P NMR (400 MHz, $CDCl_3$) δ: −6.20 ppm. HRMS (ESI): m/z 930.3125 $[M+Na]^+$ ($[C_{52}H_{50}N_3O_{10}PNa]$ = 930.3127).

A three-neck flask was chilled to −15 °C in an ice bath saturated with sodium chloride. Phosphotriester **6** (20 mg, 0.022 mmol) and 10% Pd/C (2 mg, 0.002 mmol Pd) were added, and a septum was placed in the center neck. A flow control adapter, with a Teflon stopcock and ground glass joint, was secured to one neck of the flask to enable attachment of either vacuum tubing or a balloon. The final neck was covered with a septum, an Ar(g) line was affixed, and the flask was flushed with Ar(g). Methanol (10 ml) was added, and the solution was allowed to cool. The flask was evacuated with a vacuum pump before attachment of a balloon filled with H_2(g). Evacuation, followed by reintroduction of H_2(g), was repeated two more times. The reaction was allowed to stir, covered in foil, under H_2(g) for 2 h. Reaction progress was monitored by TLC (7:1:1:1 EtOAc/H_2O/AcOH/MeOH). On completion, the palladium was rapidly removed by filtration through a pad of celite. Ammonium acetate (7.0 mg, 0.091 mmol) was added to the filtrate, and the solvent was removed under reduced pressure. The residue was purified by column chromatography using Sephadex LH-20 as the stationary phase and 1:1 MeOH/H_2O as the mobile phase. The product-containing fractions were combined, and the organic solvent was removed under reduced pressure. Water was removed by lyophilization to yield substrate **1** as a white powder (11 mg, 66%). ^{1}H NMR (400 MHz, CD_3OD) δ: 8.00 (d, J = 7.3 Hz, 1H), 7.78–7.72 (m, 1H), 7.71–7.66 (m, 1H), 7.56 (d, J = 1.3 Hz, 1H), 7.45 (d, J = 1.9 Hz, 1H), 7.33 (s, 1H), 7.16 (d, J = 7.2 Hz, 1H), 7.09 (dd, J = 8.5, 1.9 Hz, 1H), 6.95 (dd, J = 9.2, 1.3 Hz, 1H), 6.60 (d, J = 8.5 Hz, 1H), 6.54 (d, J = 8.5 Hz, 1H), 6.50 (s, 1H), 3.70 (t, J = 4.6 Hz, 4H), 3.52 (t, J = 4.5 Hz, 4H), 2.94 (s, 2H), 2.40 (s, 3H), 2.14 (s, 3H), 1.74 ppm (s, 6H). ^{13}C NMR (400 MHz, CD_3OD) δ: 174.3, 171.5, 157.4, 154.5, 153.1, 152.7, 144.4, 143.7, 142.5, 138.6, 137.3, 136.7, 131.4, 131.2, 130.4, 129.0, 128.7, 125.6, 125.3, 121.0, 117.4, 117.2, 114.8, 114.7, 114.0, 108.9, 108.6, 84.8, 67.7, 50.8, 45.6, 42.4, 33.9, 26.0, 20.5 ppm. ^{31}P NMR (400 MHz, CD_3OD) δ: −4.12 ppm. HRMS (ESI): m/z 726.2245 $[M-H]^-$ ($[C_{38}H_{37}N_3O_{10}P]$ = 726.2222).

Spectroscopic methods

Absorption measurements were made with a Cary model 50 spectrometer from Varian. Fluorometric measurements were made with a QuantaMaster1 photon-counting spectrofluorometer from Photon Technology International equipped with sample stirring. Stock solutions of rhodamine **4** [11] and *p*-nitrophenol (Aldrich Chemical, >99%) were in dimethyl sulfoxide (DMSO), and stock solutions of substrate **1** were in MeOH. Stock solutions of monosodium phosphate (Fluka Chemical, >99%) and *p*-nitrophenyl phosphate (**5**, Aldrich Chemical, >97%) were in 0.10 M Mops (pH 8.0) containing NaCl (0.50 M). Stock solutions were diluted such that the final organic solvent concentration did not exceed 1% (v/v) for alkaline phosphatase assays. Mops buffers were adjusted to the appropriate pH by adding either 1.0 M HCl or 1.0 M NaOH. *Escherichia coli* alkaline phosphatase (2 × 47 kDa [17]) was obtained from Sigma–Aldrich (product no. P4069) as a solution in buffered aqueous glycerol. All assays and standard curves were performed in triplicate, and uncertainties were expressed as standard deviations.

*Fluorometric assay with substrate **1***

Substrate **1** was diluted to appropriate concentrations and added to 2.0 ml of Mops buffer (pH 8.0). Reactions were initiated by the addition of alkaline phosphatase to a final concentration of 13 ng ml^{-1} (0.14 nM). Product formation was measured by fluorescence (λ_{ex} = 496 nm, λ_{em} = 520 nm). Fluorescence units were converted to product concentration by using a standard curve made with rhodamine **4**. Initial velocities were calculated ensuring that the total product concentration did not exceed 0.5 μM.

Rate-determining step in fluorogenesis

For substrate **1** to be useful in evaluating alkaline phosphatase activity, the rate-determining step for fluorogenesis must be the enzyme-catalyzed hydrolysis step, not the spontaneous lactonization step. The rate constant for trimethyl lock lactonization had been measured previously [16], but not in the context of a continuous assay for an enzyme-catalyzed reaction. Accordingly, we used two distinct assays to assess whether the rate of fluorogenesis reports on alkaline phosphatase activity.

*Chromogenic assay with substrate **1** and p-nitrophenyl phosphate at pHs 7.0 and 8.0*

Substrate **1** and *p*-nitrophenyl phosphate were diluted to appropriate concentrations and added to 1.0 ml of Mops buffer at pH 7.0 or 8.0. Reactions were initiated by the addition of alkaline phosphatase to a final concentration of 25 ng ml^{-1} (0.27 nM). Product formation was measured by the absorbance at 496 nm of rhodamine **4** and by that at 410 nm of *p*-nitrophenol (Scheme 1). Extinction coefficients were obtained from standard curves at pH 7.0 or 8.0.

*Malachite green assay with substrate **1***

Malachite green color reagent was prepared essentially as described previously [18]. Briefly, concentrated sulfuric acid (60 ml) was added to water (300 ml), and the resulting solution was cooled to room temperature. Malachite green oxalate (440 mg, 0.95 mmol) was dissolved in this solution. On the day of

its use, the color reagent was made by adding 2.5 ml of 7.5% (w/v) ammonium molybdate to 10 ml of the malachite green solution. Due to the low concentrations of inorganic phosphate generated during the assay, surfactant was omitted from this reagent because the color development reaction at phosphate concentrations of less than 10 μM was slow in the presence of surfactant [18].

Substrate **1** was dissolved in 1.8 ml of 0.10 M Mops (pH 8.0) containing NaCl (0.50 M). Alkaline phosphatase was added to a final concentration of 25 ng ml^{-1} (0.27 nM). The production of rhodamine **4** was monitored by its absorbance at 496 nm ($t = 0$ and 360 s). The production of phosphate was determined by removing aliquots (800 μl) from the reaction mixture ($t = 0$ and 600 s), quenching with 200 μl of color reagent in a new cuvette, and reading the absorbance at 630 nm after 3 min to allow the color to develop completely. Extinction coefficients were determined by generating standard curves for rhodamine **4** (0.05–3.0 μM) and monosodium phosphate (0.2–6.2 μM).

Results and discussion

*Synthesis of substrate **1***

Our strategy for the synthesis of a fluorogenic substrate for alkaline phosphatase is shown in Scheme 2. We had described rhodamine **4** previously [11]. Acid **5** was synthesized by a known procedure [16]. Our attempts to couple the poorly nucleophilic rhodamine **4** with sterically hindered acid **5** failed with standard carbodiimides, mixed anhydrides, and acid chlorides. Only acid chloride formation in situ using an α-chloroenamine under neutral conditions [19,20], followed by the addition of morpholinourea rhodamine and pyridine, led to successful coupling. This reaction produced an acceptable yield of 52% despite the poor solubility of morpholinourea rhodamine in dichloromethane. The benzyl protecting groups were removed by hydrogenolysis in methanol, and substrate **1** was purified as its diammonium salt.

Fluorometric assay for alkaline phosphatase

A Michaelis–Menten kinetic analysis of catalysis by alkaline phosphatase was performed using substrate **1** (Fig. 1). The hydrolysis of **1** yields equimolar inorganic phosphate, dihydrocoumarin **3**, and rhodamine **4** (Scheme 1). Rhodamine **4**, which has an extinction coefficient of 48,600 M^{-1} cm^{-1} and a quantum yield of 0.49 [11], can be detected by fluorescence spectroscopy at concentrations much less than 1 μM, which is the inhibition dissociation constant of inorganic phosphate for *E. coli* alkaline phosphatase [21]. Even for the highest substrate concentrations assayed here, the highest measured product concentration reached only

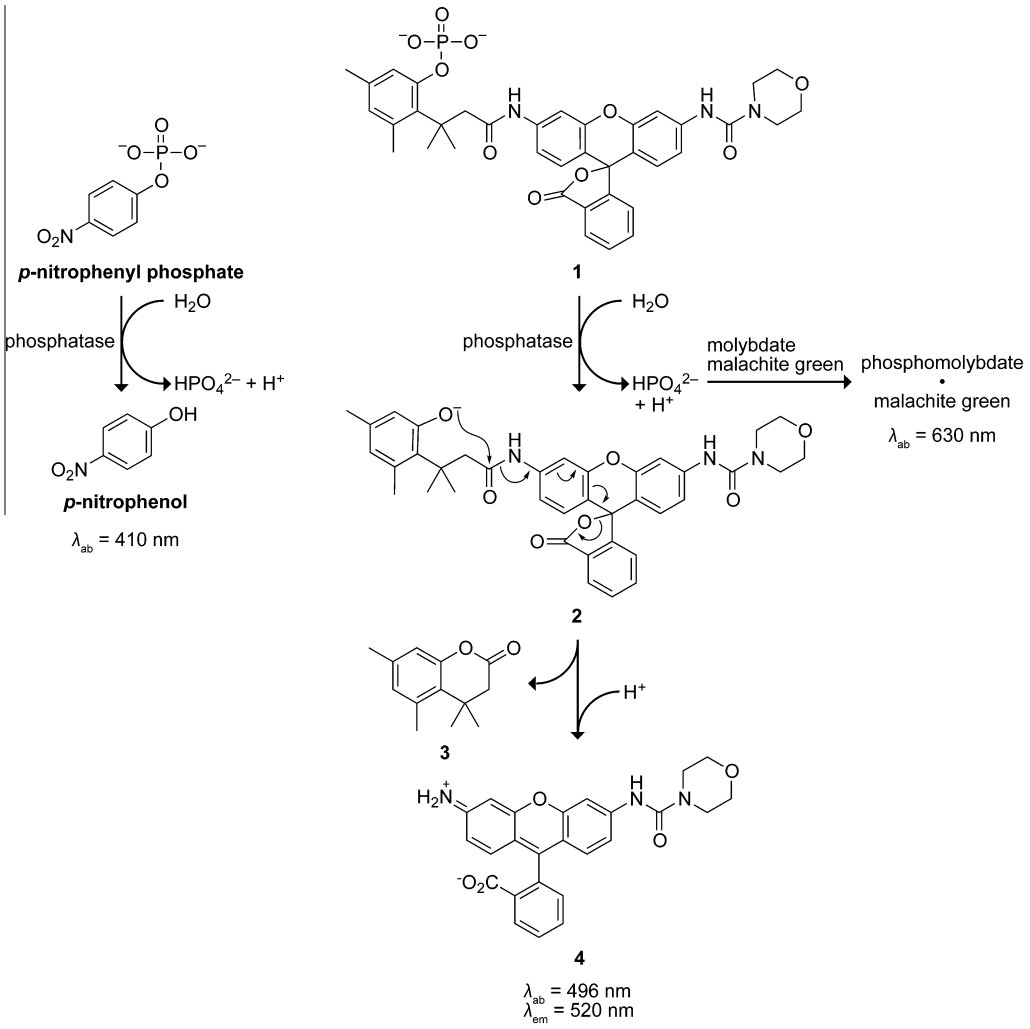

Scheme 1. Alkaline phosphatase substrates. Unmasking of trimethyl lock substrate **1** with alkaline phosphatase requires two steps: an enzymatic step with phosphatase and a chemical lactonization step. Comparison of substrate **1** with two other assays, *p*-nitrophenyl phosphate and malachite green, determined that the enzymatic step is rate-determining.

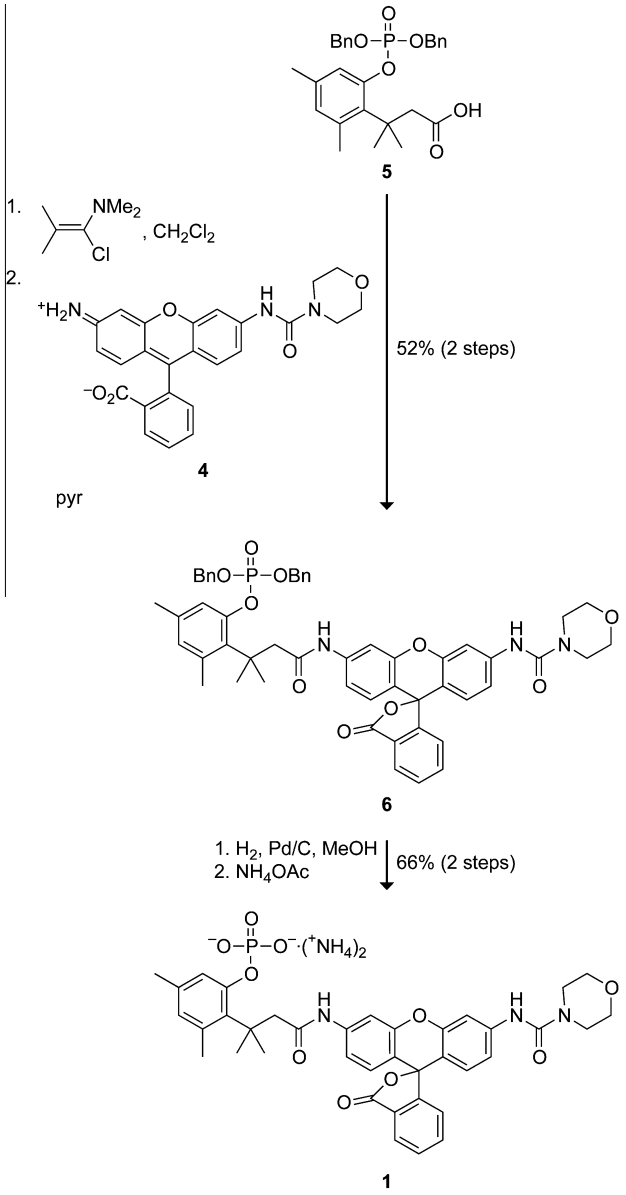

Scheme 2. Route for synthesis of substrate **1**.

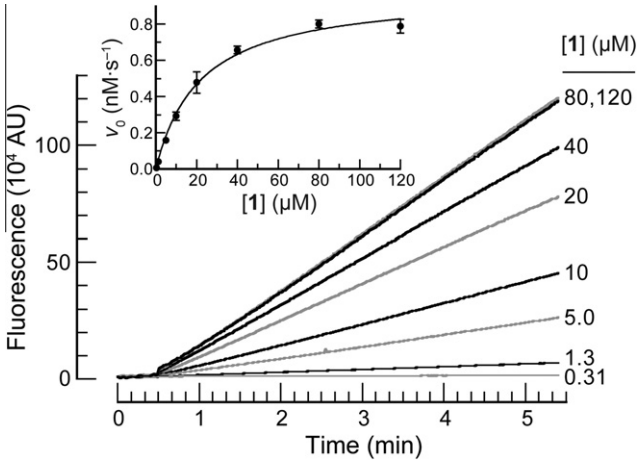

Fig.1. Catalysis of hydrolysis of substrate **1** by alkaline phosphatase, as monitored by fluorescence spectroscopy. Assays were performed in 0.10 M Mops buffer (pH 8.0) containing NaCl (0.50 M), substrate **1** (0.31–120 μM), and *E. coli* alkaline phosphatase (13 ng ml^{-1}, which was added at t = 30 s). Reactions were monitored by the change in fluorescence at λ_{em} = 520 nm on excitation at λ_{ex} = 496 nm. Michaelis–Menten analysis (inset): k_{cat} = (7.3 ± 0.4) s^{-1} and k_{cat}/K_M = (3.3 ± 0.5) × 10^5 M^{-1} s^{-1}. Uncertainties are expressed as the standard deviation of three experiments.

0.3 μM. Thus, the high sensitivity of substrate **1** can provide accurate kinetic data by ensuring that inorganic phosphate does not attain inhibitory concentrations.

*Rate-determining step for alkaline phosphatase-catalyzed hydrolysis of substrate **1***

As shown in Scheme 1, two steps are required for the generation of fluorescence from substrate **1**: (i) enzyme-catalyzed P–O bond cleavage to release phenol **2** and inorganic phosphate and (ii) nonenzymatic lactonization of phenol **2** with concomitant release of morpholinourea rhodamine **4**. For substrate **1** to provide a valid report of alkaline phosphatase activity, the rate of nonenzymatic lactonization must be faster than that of enzyme-catalyzed P–O bond cleavage.

We used two methods to verify that the rate-determining step of fluorescence generation from substrate **1** is indeed the enzymatic step. First, we compared the effect of pH on the steady-state kinetic parameters for the production of rhodamine **4** with that for the production of *p*-nitrophenol from *p*-nitrophenyl phosphate (which does not entail a nonenzymatic step). Next, we measured independently the rate of fluorogenesis and the rate of inorganic phosphate production.

*Comparison of substrate **1** with p-nitrophenyl phosphate at pHs 7.0 and 8.0*

In addition to its utility as a latent fluorophore, substrate **1** can also be employed as a latent chromophore because rhodamine **4** has robust absorbance at 496 nm. Alkaline phosphatase is often assayed by monitoring its ability to catalyze the hydrolysis of another latent chromophore, *p*-nitrophenyl phosphate, to form *p*-nitrophenol (Scheme 1), which has a conjugate base with absorbance at 410 nm. Unlike with substrate **1**, P–O bond cleavage of *p*-nitrophenyl phosphate generates a chromophore in a single step [3]. Accordingly, a comparison of these two chromogenic substrates can be used to assess the rate-determining step for the production of rhodamine **4** from substrate **1**.

The steady-state kinetic parameters for the hydrolysis of different aryl phosphates by *E. coli* alkaline phosphatase determined at pH 7.0 should vary in a constant manner when determined at pH 8.0 [3,21,22]. This variance would be confounded if lactonization, rather than hydrolysis, were rate-determining for fluorogenesis from substrate **1**. The value of k_{cat} for the alkaline phosphatase-catalyzed hydrolysis of *p*-nitrophenyl phosphate is known to increase by approximately 3-fold from pH 7.0 to 8.0 [17]. Accordingly, we assayed the ability of alkaline phosphatase to generate chromophores from substrate **1** and *p*-nitrophenyl phosphate at pHs 7.0 and 8.0.

We found that the alkaline phosphatase-catalyzed hydrolysis of both substrate **1** and *p*-nitrophenyl phosphate varied with pH (Table 1). Importantly, both substrates showed approximately a 3-fold increase in k_{cat} and a 5-fold increase in K_M at pH 8.0 compared with pH 7.0. This correlation suggests that the enzymatic step limits the rate of fluorogenesis from substrate **1**. There is, however, a caveat.

Lactonization of phenol **2** required deprotonation of the phenolic hydroxyl group (pK_a ≈ 10.3 [15]; Scheme 1). A pH shift from 7.0 to 8.0 results in a 10-fold increase in the deprotonated form and

Table 1
Alkaline phosphatase assay of *p*-nitrophenyl phosphate and substrate **1** at pHs 7.0 and 8.0.

	p-Nitrophenyl phosphate			Substrate **1**		
	k_{cat} (s^{-1})	K_M (μM)	k_{cat}/K_M ($M^{-1}\,s^{-1}$)	k_{cat} (s^{-1})	K_M (μM)	k_{cat}/K_M ($M^{-1}\,s^{-1}$)
pH 8.0	118 ± 2	4.6 ± 0.4	$(2.6 \pm 0.2) \times 10^7$	13 ± 1	26 ± 6	$(5.0 \pm 1.2) \times 10^5$
pH 7.0	35 ± 1	1.0 ± 0.1	$(3.4 \pm 0.5) \times 10^7$	4.7 ± 0.5	5.4 ± 2.5	$(8.6 \pm 4.2) \times 10^5$
Ratio	3.3 ± 0.1	4.5 ± 0.8	0.75 ± 0.13	2.9 ± 0.4	4.9 ± 2.6	0.58 ± 0.32

Note: Kinetic parameters (± standard deviations) were determined by monitoring reactions in 0.10 M Mops buffer containing NaCl (0.50 M) and *E. coli* alkaline phosphatase (25 ng·ml^{-1}) with spectrophotometry (*p*-nitrophenyl phosphate, $\lambda = 410$ nm; substrate **1**, $\lambda = 496$ nm).

should increase the rate of lactonization by 10-fold. Consequently, some of the observed approximately 3-fold increase in k_{cat} at pH 8.0 (Table 1) could be due to an increase in the rate of lactonization. Accordingly, we devised an assay to monitor the hydrolysis and lactonization reactions of substrate **1** simultaneously.

Comparison of fluorogenesis and inorganic phosphate production

Alkaline phosphatase catalyzes the hydrolysis of substrate **1** to inorganic phosphate and phenol **2**, neither of which has measurable absorbance. Malachite green, however, forms a complex with phosphate and molybdate (Fig. 1), generating an intense green color [18,23,24]. We found that the concentrations of inorganic phosphate (malachite green assay) and rhodamine **4** (chromogenesis assay) increased at the same rate on hydrolysis of substrate **1** by alkaline phosphatase (Fig. 2). These data, like the comparative pH-dependent rates, indicate that the enzymatic step is rate-determining for fluorogenesis from substrate **1** and validate this substrate as a reporter of alkaline phosphatase activity.

Assays of other phosphatases

Finally, we note that substrate **1** could be suitable for assays of other phosphatases, including those of clear medical importance. These phosphatases, which include calcineurin, PP2A, PP5, and PTEN [25–27], do not necessarily have low K_i values for inorganic phosphate. Still, assays of their enzymatic activity could benefit from the high sensitivity provided by substrate **1**.

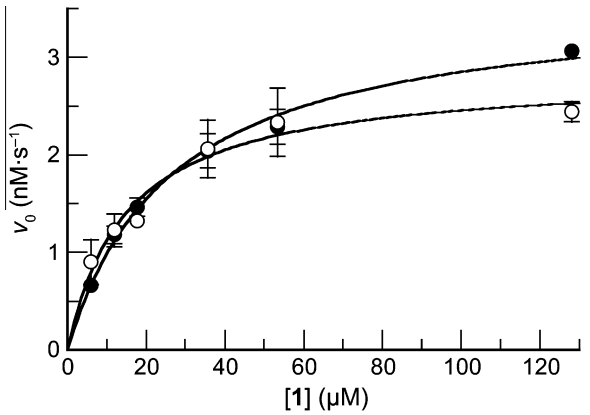

Fig.2. Catalysis of hydrolysis of substrate **1** by alkaline phosphatase, as monitored by absorbance spectroscopy and a malachite green assay for inorganic phosphate. Shown are Michaelis–Menten plots for the serial dilution of substrate **1** (128 → 5.9 μM) with *E. coli* alkaline phosphatase (25 ng ml^{-1}) in 0.10 M Mops buffer (pH 8.0) containing NaCl (0.50 M). Product formation was measured by the absorbance of rhodamine **4** at 496 nm (●), $k_{cat} = (13 \pm 1)\,s^{-1}$ and $k_{cat}/K_M = (5.0 \pm 1.2) \times 10^5\,M^{-1}\,s^{-1}$, or by a malachite green assay for inorganic phosphate (○), $k_{cat} = (10 \pm 2)\,s^{-1}$ and $k_{cat}/K_M = (6.9 \pm 3.6) \times 10^5\,M^{-1}\,s^{-1}$. Uncertainties are expressed as the standard deviation of three experiments.

Conclusions

We have generated a sensitive fluorometric substrate that can be used to assay alkaline phosphatase activity without the risk of product inhibition by inorganic phosphate. We showed that the rate-determining step of fluorogenesis from this substrate is enzyme-catalyzed hydrolysis. We anticipate that substrate **1** would be useful for other phosphatases as well and could achieve widespread use in ELISAs and other assays that employ phosphatases.

Acknowledgments

We are grateful to L.D. Lavis, S.S. Chandran, E.L. Myers, V. Shakhnovich, K.H. Jensen, and W.W. Cleland for contributive discussions. This work was supported by Grant R01 CA073808 from the National Institutes of Health (NIH) and made use of the National Magnetic Resonance Facility at Madison (NMRFAM), which is supported by NIH grants P41RR02301 (BRTP/NCRR) and P41GM66326 (NIGMS). The purchase of the Waters (Micromass) Autospec in 1994 was funded in part by grant CHE-9304546 from the National Science Foundation (NSF) to the Department of Chemistry at the University of Wisconsin–Madison.

References

[1] J.E. Coleman, Structure and mechanism of alkaline phosphatase, Annu. Rev. Biophys. Biomol. Struct. 21 (1992) 441–483.
[2] J.L. Millán, Alkaline phosphatases: structure, substrate specficitiy, and functional relatedness to other members of a large superfamily of enzymes, Purinergic Signal. 2 (2006) 335–341.
[3] W.W. Cleland, A.C. Hengge, Enzymatic mechanisms of phosphate and sulfate transfer, Chem. Rev. 106 (2006) 3252–3278.
[4] B. Porstmann, T. Porstmann, E. Nugel, U. Evers, Which of the commonly used marker enzymes gives the best results in colorimetric and fluorimetric enzyme immunoassays: horseradish peroxidase, alkaline phosphatase, or β-galactosidase?, J Immunol. Methods 79 (1985) 27–37.
[5] S.L. Snyder, I.B. Wilson, Phosphoramidic acids: a new class of nonspecific substrates for alkaline phosphatase from *Escherichia coli*, Biochemistry 11 (1972) 1616–1623.
[6] Z. Huang, Q. Wang, H.D. Ly, A. Gorvindarajan, J. Scheigetz, R. Zamboni, S. Desmarais, C. Ramachandran, 3,6-Fluorescein diphosphate: a sensitive fluorogenic and chromogenic substrate for protein tyrosine phosphatases, J. Biomol. Screening 4 (1999) 327–334.
[7] D. Robinson, P. Willcox, 4-Methylumbelliferyl phosphate as a substrate for lysosomal acid phosphatase, Biochim. Biophys. Acta 191 (1969) 183–186.
[8] M. Ceresole, Verfahren zur Darstellung von Farbstoffen aus der Gruppe des Meta-amldophenol-Phtaleïns, D.R. patent 44002 (1887).
[9] L.D. Lavis, R.T. Raines, Bright ideas for chemical biology, ACS Chem. Biol. 3 (2008) 142–155.
[10] S.S. Chandran, K.A. Dickson, R.T. Raines, Latent fluorophore based on the trimethyl lock, J. Am. Chem. Soc. 127 (2005) 1652–1653.
[11] L.D. Lavis, T.-Y. Chao, R.T. Raines, Fluorogenic label for biomolecular imaging, ACS Chem. Biol. 1 (2006) 252–260.
[12] L.D. Lavis, T.-Y. Chao, R.T. Raines, Latent blue and red fluorophores based on the trimethyl lock, ChemBioChem 7 (2006) 1151–1154.
[13] M.M. Yatzeck, L.D. Lavis, T.-Y. Chao, S.S. Chandran, R.T. Raines, A highly sensitive fluorogenic probe for cytochrome P450 activity in live cells, Bioorg. Med. Chem. Lett. 18 (2008) 5864–5866.
[14] S. Milstien, L.A. Cohen, Stereopopulation control: I. Rate enhancement in the lactonizations of *o*-hydroxyhydrocinnamic acids, J. Am. Chem. Soc. 94 (1972) 9158–9165.

[15] R.T. Borchardt, L.A. Cohen, Stereopopulation control: II. Rate enhancement of intramolecular nucleophilic displacement, J. Am. Chem. Soc. 94 (1972) 9166–9174.
[16] M.G. Nicolaou, C. Yuan, R.T. Borchardt, Phosphate prodrugs for amines utilizing a fast intramolecular hydroxy amide lactonization, J. Org. Chem. 61 (1996) 8636–8641.
[17] L. Sun, D.C. Martin, E.R. Kantrowitz, Rate-determining step of *Escherichia coli* alkaline phosphatase altered by the removal of a positive charge at the active center, Biochemistry 38 (1999) 2842–2848.
[18] A.A. Baykov, O.A. Evtushenko, S.M. Avaeva, A malachite green procedure for orthophosphate determination and its use in alkaline phosphatase-based enzyme immunoassay, Anal. Biochem. 171 (1988) 266–270.
[19] B. Haveaux, A. Dekoker, M. Rens, A.R. Sidani, J. Toye, L. Ghosez, α-Chloroenamines, reactive intermediates for synthesis: 1-chloro-*N*,*N*,2-trimethylpropenylamine, Org. Synth. 59 (1979) 26–34.
[20] M.N. Levine, L.D. Lavis, R.T. Raines, Trimethyl lock: a stable chromogenic substrate for esterases, Molecules 13 (2008) 204–211.
[21] P.J. O'Brien, D. Herschlag, Alkaline phosphatase revisited: hydrolysis of alkyl phosphates, Biochemistry 41 (2002) 3207–3225.
[22] W.E. Hull, S.E. Halford, H. Gutfreund, B.D. Sykes, ^{31}P nuclear magnetic resonance study of alkaline phosphatase: the role of inorganic phosphate in limiting the enzyme turnover rate at alkaline pH, Biochemistry 15 (1976) 1547–1561.
[23] K. Itaya, M. Ui, A new micromethod for the colorimetric determination of inorganic phosphate, Clin. Chim. Acta 14 (1966) 361–366.
[24] L. Chang, E.B. Bertelsen, S. Wisén, E.M. Larsen, E.R. Zuiderweg, J.E. Gestwicki, High-throughput screen for small molecules that modulate the ATPase activity of the molecular chaperone DnaK, Anal. Biochem. 372 (2008) 167–176.
[25] R.E. Honkanen, T. Golden, Regulators of serine/threonine protein phosphatases at the dawn of a clinical era, Curr. Med. Chem. 9 (2002) 2055–2075.
[26] C. Eng, PTEN: one gene, many syndromes, Hum. Mutat. 22 (2003) 183–198.
[27] S. Romano, A. Di Pace, A. Sorrentino, R. Bisogni, L. Sivero, M.F. Romano, FK506 binding proteins as targets in anticancer therapy, Anticancer Agents Med. Chem. 10 (2010) 651–656.